International Journal of Mechanical and Production Engineering Research and Development (IJMPERD)
ISSN (P): 2249-6890; ISSN (E): 2249-8001
Vol. 9, Issue 2, Apr 2019, 827-840

Original Article

THE EFFECT OF TEMPERATURE AND THERMODYNAMICS STUDIES ON THE REMOVAL OF HEAVY METAL BY USING ADSORBENT

A. MUTHULAKSHMI[1,2] & R. BASKARAN[3]

[1]*Department of Chemical Engineering, Sathyabama University, Chennai, Tamil Nadu, India*

[2]*Department of Biotechnology, Jeppiaar Engineering College, Chennai, Tamil Nadu, India*

[3]*Department of Chemical Engineering, St. Joseph's Engineering College, Chennai, Tamil Nadu, India*

ABSTRACT

The need for waste water treatment has intensified in the recent past with the advent of industrial revolution. The major contaminants of water are heavy metals of which chromium, used in leather and electroplating industries is of major concern due to its chronic toxicity. Chromium contamination affects the portability of water and the life forms in it. Hence treatment of chromium contaminated water is necessary. Adsorption using low cost adsorbents proves advantageous due to their efficiency and low cost. In this study, we evaluated the chromium adsorption efficiency of Phyllanthus emblica leaves. The parameters which affect adsorption such as pH, adsorbent concentration, adsorbate concentration, time of contact were optimized to improve the efficiency. The results indicate adsorption had a linear relation with time. The highest chromium adsorption of 58.03 mg/g of absorbent was observed at pH 4 after 2 h of constant stirring. The SEM image of the plant material appeared like a sieve holding up the chromium ions after adsorption. FTIR of the plant material had a high percentage of OH^- functional group and organic functional groups C-H and C=C. After adsorption, there was an increase in transmittance of 568 cm^{-1} peak and 3409 cm^{-1} peak, which corresponds to the metallic bond and OH^{-1} functional group respectively. The study implies that the leaves of Phyllanthus emblica are potential chromium adsorbents and can be explored for industrial use.

KEYWORDS: Chromium, Adsorption, Phyllanthus Emblica, SEM & FTIR

Received: Feb 09, 2019; **Accepted**: Mar 01, 2019; **Published**: Apr 01, 2019; **Paper Id**.: IJMPERDAPR201980

1. INTRODUCTION

The industrial revolution has increased the discharge of heavy metal contaminants into the environment (Balan et al. 2009). These industrial discharges have to be treated before letting out into the surroundings. However, highly toxic quantities of heavy metals are let out along with the uncontrolled and untreated industrial water. Heavy metals due to their toxicity, persistency and bioaccumulating nature are of specific concern as they are highly dangerous if accumulated by any living organism (Aksu and Akpinar 2001). Among heavy metals, the environmental pollution by Chromate (Cr^{6+}, CrO_4^{2-}) is regarded as a priority pollutant by the US EPA. Chromium is a potential mutagen and carcinogen. The Cr^{6+} form is considered more toxic than Cr^{3+} form (Chwastowski and Kołoczek 2013; Yuan et al. 2010). The toxicity of chromium arises from the redox reactions such as single electron reduction by flavoenzymes, leading to the formation of Cr (V). This sub-sequentially initiates formation of reactive oxygen species (ROS) leading to damage of phospholipids, proteins and DNA (Stearns and Wetterhahn 1994; Levina and Lay 2004).

The sources of Chromium include leather tanning, electroplating, cement, dyeing, wood preservatives,

paint and pigments, textile dyeing and steel fabrication industries (Hadjmohammadi et al. 2011). Leather tanning is the major source of chromium where chromium sulfate is preferred over vegetable substances for reducing the processing time, cost and for obtaining light colour, high stability and mechanical resistance, dyeing suitability and hydrothermic resistance (Gebrehawaria et al. 2015). Only 60-80% of chromium used in the leather industry is taken up during the process while the rest is usually discharged in effluents. The maximum permitted level of trivalent chromium is 5.00 mg/L and for hexavalent chromium is 0.05 mg/L. Though the limit of chromium discharge in aqueous effluents is limited depending on the country, much higher concentrations of upto 200000 mg/L is being discharged. Thus, posing a serious threat to the environment and requires immediate remediation of chromium containing water.

Various remediation methods are in existence, but are limited by high capital and regeneration costs. Biosorption has proven to be promising for the removal of heavy metals (Oboh et al. 2009). The major advantage of this technique is its efficiency. Biosorption can remove high concentrations of heavy metals at low cost, with the possibility of adsorbent recovery. Relatively low cost, abundant and environmental friendly materials such as plant biomass, agricultural waste, algal biomass are the ones usually utilized for bioadsorption (Fiol et al. 2008; Gupta et al. 2010). In general, the metal ions from the aqueous medium are transferred to the surface of the bulk biosorbent due to the surface charge (Pehlivan et al. 2012, Mishra et al. 2015). Relatively large number of materials has been studied for their biosorption efficiency. However, for adsorption of high concentrations of chromium upto 1000 mg/L from synthetic effluents, only a few reports are available (Muthulakshmi et al. 2016a, 2016b).

The present study was conducted to analyse the efficiency of *Phyllanthus emblica* leaves for biosorption of high concentrations of Chromium in real time effluents. A number of studies have emphasized on the factors affecting adsorption process such as contact time, solution pH, adsorbate concentration, adsorbent concentration, etc. (Farooq et al. 2010). Hence, the purpose of the study is to establish an optimized condition for adsorption of chromium by *Phyllanthus emblica* and further study the functional groups involved in adsorption process of chromium.

2. MATERIALS AND METHODS

2.1 Sample Collection and Preparation

Phyllanthus emblica leaves were collected from Chennai, Tamil Nadu, India. The collected leaf samples were washed and shade dried in the room temperature for one week. The samples were then pulverized and sieved to obtain uniform size of 300µm (ASTM-E11 No.50). The sieved samples were used for the adsorption experiments.

2.2 Preparation of Effluent Sample and Optimization Studies

Effluent were collected from Chennai, Tamil Nadu, India and analysed for the concentration of chromium using the DPC method (APHA, 2005). The purple coloured solution formed was read after 20 min at 540 nm using UV Visible spectroscopy. The stock solution was prepared by diluting the effluent to an initial adsorbate concentration of 2000 mg/L. The stock was diluted to form 250, 500, 750 and 1000mg/L concentrations of chromium. Batch adsorption studies were done with 100ml of effluent containing chromium concentrations of 250, 500, 750 and 1000mg/L and 1g of adsorbent. The samples after adsorption were filtered using Whattman filter paper and the metal ion concentrations in the filtrate was analysed by DPC method. The amount of chromium adsorbed was calculated using the following equation:

$$q = (C_0 - Ce)\ V/\ W$$

Where, q amount of Cr (VI) adsorbed by the adsorbent (mg/g),

C_0 is the initial concentration of Cr (VI) and Ce is the concentration of chromium at equilibrium (mg/ml),

V is the initial volume of chromium solution (ml), and

W is the weight of the adsorbent (g).

Adsorbate concentration for further studies was selected and the optimizations of other parameters were performed. The parameters optimized include pH, agitation time and adsorbent concentration. The pH of the solution was varied from pH 2 to pH 6 in increments of 1 using 1N HCl. The absorbent at various weight percentages were analysed for adsorption efficiency (0.5, 1.0, 1.5 and 2 %) at all pH conditions studied. The samples were drawn at different time intervals such as 30, 60, 90 and 120min and the concentration of chromium was evaluated for all the samples.

2.3 Characterization of Adsorption Process

The leaf samples before and after adsorption were imaged using Scanning Electron Microscope (IITM, Chennai). The SEM images of plant material before and after adsorption are presented in samples 2a and 2b-d respectively. The FTIR spectra was analysed by KBr pellet technique in the spectra range of wavenumber 400-4000 cm-1 for the effluent and leaf samples before and after adsorption. The FTIR spectra of plant material, chromium effluent and plant material after adsorption are presented in figure 3a, 3b and 3c respectively.

3. RESULTS AND DISCUSSIONS

3.1 Optimization of Process Parameters

The adsorption of Chromium using Phyllanthus emblica was studied and the factors affecting adsorption such as pH, adsorbent concentration and contact time were optimized. One of the important control factors in any adsorption study is pH, as it has an influence on the surface properties of adsorbent as well as the ionic form of the metal ion in solution (Mahajan and Sud 2011). The pH of the solution is critical as it affects the degree of metal ion speciation and adsorbent's active functional sites dissociation (Azouaoua et al. 2010). Chromium's isoelectric point is 6.2, hence the optimization was carried out in the pH range 2-6, since above this Cr6+ starts to precipitate; therefore higher pH was not studied. Each pH was studied with different adsorbent dosage and the effect of contact time was evaluated for each sample. The result for optimization of adsorption is shown in figures 1 (a-e).

The optimization of solution pH revealed that adsorption was maximum at pH 4 at 120 min with 1 g of adsorbent per 100 ml of chromium solution. With the increase in hydroxyl ion concentration, the adsorption efficiency decreased similar to previous reports (Mahajan and Sud 2011, Mishra et al 2015). The speciation of metal ions and dissociation of active functional sites present on the biosorbent is governed by pH of the aqueous solution (Azouaoua et al. 2010; Malkoc et al. 2006). Adsorption of metal ions depends critically on the solution pH. The optimum pH not only varies according to metal ions, but also according to the kind of biomass used (Ucun et al. 2002). This can be observed from our previous reports where optimum pH varies between pH 3.0 and pH 5.0 (Muthulakshmi 2016a, b & 2017). The anionic form of chromium in aqueous solution such as chromate CrO_4^{2-}, dichromate $Cr_2O_7^{2-}$, or hydrogen chromate $HCrO_4^-$ is determined by the pH. (Dakiky et al. 2002). Above isoelectric point, Chromium exists as CrO_4^{2-} ions, while below isoelectric point it exists mainly as $HCrO_4^-$ and $Cr_2O_7^{2-}$. $HCrO_4^-$ which predominates the solution at lower pH gets converted to other forms as the pH increases. Protonation of biosorbent surface at lower pH by H+ ions promotes the adsorption of the predominantly

occurring negatively charged $HCrO_4$- ions.

The adsorbent dosage was varied between 0.5 and 2 gm per 100 ml of solution. The amount of adsorbent is much higher than usual experiments because high concentrations of chromium are experimented in this study. The increase in adsorbent dosage in general increases the adsorption efficiency due to the increase in surface area available for adsorption (Garg et al., 2004). However, a high dosage causes overcrowding of adsorbent particles which leads to overlap of adsorption sites. In our study, the efficiency of adsorption was found to increase when the adsorbent dosage was increased from 0.5 to 1 gm. However on further increase of adsorbent dosage, the efficiency was lower, which might be due to overcrowding of adsorbent particles or redispersing of the adsorbed particles into the solution. Similar observations were made by Hadjmohammadi *et al*., 2011and Babel and Opiso, 2007. Thus the optimum concentration of adsorbent is 1 gm per 100 ml of effluent solution.

Further, the effect of contact time on adsorption was studied to establish a relation between the effect of pH, adsorbent dosage and contact time on adsorption efficiency. The contact time was varied in intervals of 30 min upto 120 min. Maximum adsorption was observed in 120 min of contact time, as the adsorption efficiency increased linearly with contact time. However, the adsorption was found to increase rapidly until 30 min. With further increase in contact time, the rate of adsorption was found to decrease significantly. This might be due to the fact that initially all the sites on the surface of biosorbent are available for adsorption and the solute concentration gradient is relatively high. Consequently with time, the vacant sites on the surface of the adsorbent gets occupied, thus decreasing the number of vacant sites and thereby the adsorption efficiency (Mezenner et al. 2009; Kaouah et al. 2014). The adsorption of chromium by *Phyllanthus emblica* leaves are presented in figure 1 a-e.

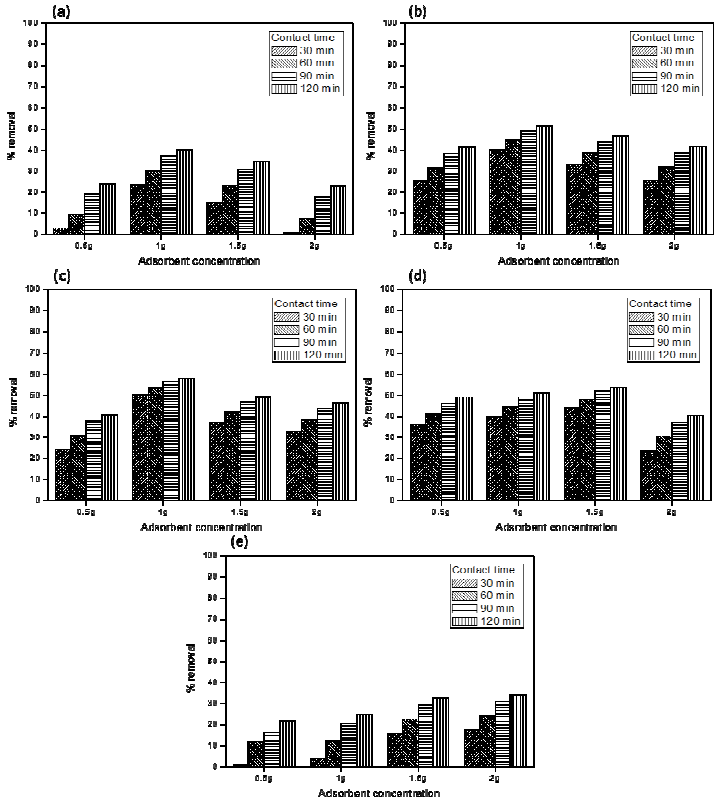

Figure 1: Optimization of Adsorbent Concentration and Contact Time at pH 2 (a), pH 3 (b) pH 3 (c), pH 5 (d) and pH 6 (e)

3.2 Scanning Electron Microscopy (SEM)

The scanning electron microscope image of plant material before and after adsorption is shown in 2a and 2b-d respectively. The SEM image of plant material before adsorption appears sieve like. While the SEM image of plant material after adsorption presented in images 2b-d show that the chromium ions being adsorbed on the surface of plant material. The images 2b-d represents the plant material after adsorption imaged at different magnifications. The chromium ions appear to be aggregated on the surface of the plant material thus forming layers. These layers appear on the surface of plant material which is visible clearly in the SEM image of the plant material after adsorption.

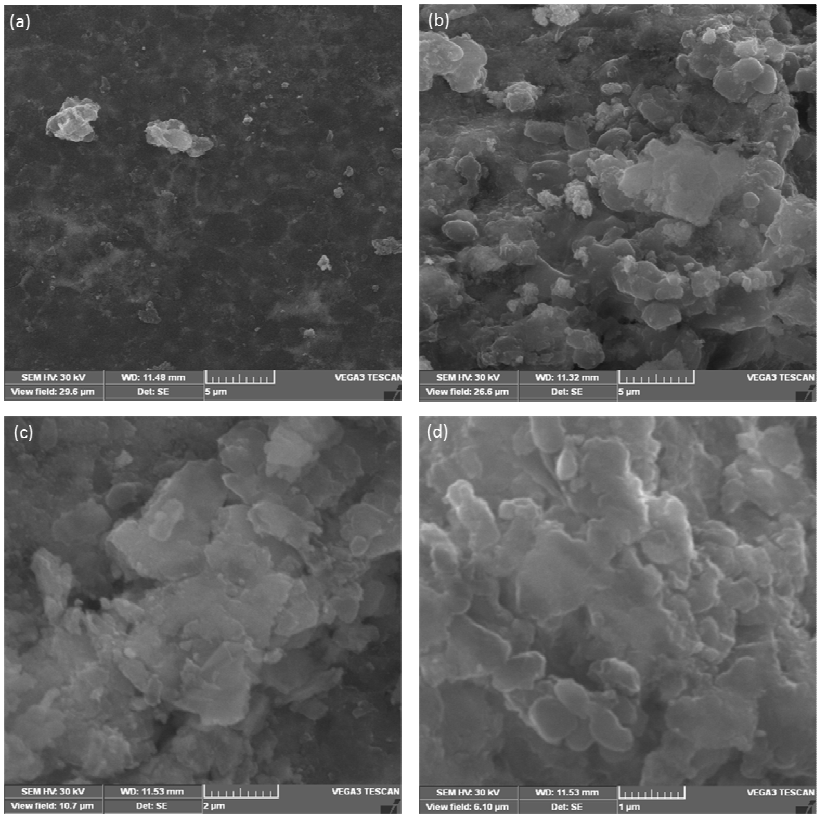

Figure 2: Scanning Electron Microscope Image of Plant Material before (a) and After Chromium Adsorption (b, c & d)

3.3 Fourier Transform Infrared Spectroscopy (FTIR)

The FTIR spectra of plant material, chromium effluent and plant material after adsorption are presented in figure 3a, 3b and 3c respectively. In figures 3a and 3c, the broad peak around 3500 cm^{-1} correspond to hydroxyl group, H-bonded OH stretching. The peak around 2950 cm^{-1} corresponds to methyl C-H symmetrical stretch. The peaks from 1225-1000 cm^{-1} correspond to the aromatic C-H out of plane bend. The peaks from 1310- 1290 cm^{-1} corresponds to vinylidene C-H in plane bend while those from 1350-1330 cm^{-1} correspond to methyne C-H bend and from 1485-1445 cm^{-1} correspond to methylene C-H bend. Peaks from 1615–1580 and 1510-1450 cm^{-1} correspond to aromatic ring stretch which is due to the phenolic groups in plants. The C-O bond occur around 1620-1780 cm^{-1} which represent both saturated and unsaturated compounds. In figure 3b, the peak around 3500 cm^{-1} corresponds to hydroxyl group. The peaks at 880 cm^{-1} and 940 cm^{-1} are characteristic peaks of Cr-O vibrations and peak at 740 cm^{-1} correspond to Cr=O vibration. The peaks at 1260, 1640 and 1860 cm^{-1} may be due to oxalate ions present in the effluent which gets physically absorbed to Chromium ions. In

figure 3c, the peak at 740 cm^{-1} could be observed. Also an additional broad peak is observed at 575 cm^{-1} which has shifted from 570 cm^{-1} in FTIR spectra of chromium effluent. These peaks indicate that chromium ions have been adsorbed on the surface of plant material, since these peaks correspond to Chromium vibrations.

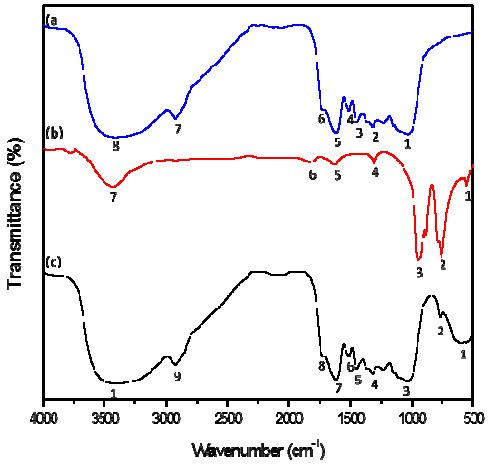

Figure 3: FTIR Spectra of Plant Material (a), Chromium Effluent (b) and Plant Material after Chromium Adsorption (c)

3.4 Adsorption Isotherms

Adsorption isotherms were studied by fixing the adsorbent concentration at 1g and by varying the adsorbate concentration. The distribution of metal ions between the liquid phase and solid phase is given by adsorption isotherms. The sorption adsorption isotherm explains the relation between the adsorbent and the sorbate at equilibrium (Langmuir 1918). Langmuir, Freundlich and Temkin adsorption models were applied to the obtained experimental data at room temperature (Gebrehawaria et al. 2015; Muthulakshmi et al. 2016). Adsorption isotherms help in identifying the suitable model which can be used for design purpose.

Langmuir adsorption isotherm validates the monolayer adsorption of the adsorbate to identical homogenous sites on the surface of the adsorbent, without any interaction between itself. Langmuir isotherm explains the adsorption in equilibrium and provides information on the maximum adsorption capacity. The Langmuir expression is given by equation 1

$$C_e/q_e = (1/bq_{max}) + (1/q_{max})C_e \quad (1)$$

Where C_e is the concentration of Chromium ions in aqueous phase. qe is the amount of chromium ions concentration at equilibrium (mg/g), q_{max} is the maximum metal uptake per unit mass of plant material (mg/g) and b is the Langmuir constant (L) which is related to energy of sorption. The parameters of the Langmuir isotherm q_{max} and b were calculated from the intercepts and slopes of the linear plots. The Langmuir constant b is related to adsorption constant and desorption constant by the equation 2

$$b = k_a/k_d \quad (2)$$

The linear graph indicates a linear relationship between the amounts of Chromium ions adsorbed per unit mass (g) of the plant material against the concentration of chromium ions remaining in the solution (mg/l). The q_{max} and b values were 62.118 mg/g and 0.01286 L/mg. The separation factor (RL) was calculated from the values of the adsorption energy

(b) and concentration at equilibrium Ce, using the equation 3. The value of separation factor R_L describes the adsorption process. If R_L=0, the adsorption is irreversible, R_L between 0 and 1 indicates adsorption is favourable, R_L=1 indicates adsorption is linear and R_L of 1 indicates that adsorption is unfavourable.

$$R_L = 1/(1 + bC_e) \quad (3)$$

The value of separation factor varied from 0.27 to 0.07 when the concentration was varied from 250 mg to 1000 mg, which is well below zero. All the values ranged from 0 to 1 which implies favourable adsorption. Further high R_L indicates that adsorption is favourable at lower concentration (Hadjmohammadi et al. 2011). The R^2 value was 0.9952, which indicates that the adsorption follows Langmuir adsorption isotherm, and there is no interaction between ions during adsorption.

Freundlich isotherm parameters were similarly calculated based on the equation 5, from the slopes and intercepts from the plot between log q_e versus log C_e. The adsorption intensity of the adsorbate by leaves is represented by equation 4.

$$q_e = k_f C^{1/n} \quad (4)$$

Where both n and k_f are Freundlich constants, 1/n is the intensity of adsorption and k_f gives the bioorption capacity (Voudrias et al., 2002). The equation 4 is linearized to equation 5 by taking log on both sides.

$$log\ q_e = log\ k_f + \frac{1}{n} log\ C_e \quad (5)$$

The R^2 value was 0.924, which is high and imply that the adsorption process follows Freundlich isotherm. The adsorption capacity (k_f) and intensity of metal ions towards the adsorbent (1/n) was found to be 23.92 and 0.1279 respectively. The adsorption on a heterogeneous surface and the exponential distribution of active sites and their energies are the basis of Freundlich isotherm and are used for calculating the parameters. The 1/n value was between 0 and 1 indicating the adsorption to be favourable (Abdullah and Prasad 2009).

The Temkin adsorption isotherm explains the relation between the adsorbent and adsorbate. Temkin et al. 1940 considers that the heat of adsorption of all molecules in monolayer will decrease linearly rather than logarithmically. Temkin isotherm is given by equation 6. The slope and intercept of the plot between q_e against ln C_e gives uniform distribution of binding energies (B) and constant A_T.

$$q_e = \frac{RT}{b} \ln(A_f C_e)$$

$$q_e = \frac{RT}{b} \ln(A_f) + \frac{RT}{b} \ln(C_e) \text{ Considering } B = \frac{RT}{b_T}$$

$$q_e = B \ln(A_f) + B \ln(C_e) \quad (6)$$

where, A_f =Temkin isotherm equilibrium binding constant (L/g); b_r = Temkin isotherm constant; R = universal gas constant (8.314J/mol/K); T = Temperature at 298K; B = Constant related to heat of sorption (J/mol).

From the plot of ln C_e Vs q_e, the R^2 value was found to be 0.9108, B was 6.714 J/mol and A_f was 5.455 L/g. The Temkin isotherm constant b_r value was 348.994 calculated using standard values of gas constant and T. The R^2 value

indicates that the equilibrium data is better fitted in Langmuir isotherm than in Freundlich and Temkin adsorption isotherm.

The parameters for plotting Langmuir, Freundlich and Temkin adsorption isotherms for *P. emblica* is given in table 1 and Langmuir, Freundlich and Temkin isotherm constants is presented in table 2.

Table 1: Parameters Used for Plotting Langmuir, Freundlich and Temkin Adsorption Isotherms of *P. emblica*

Co (mg/L)	Qe (mg/L)	Ce (mg/L)	1/Co	1/Qe	1/Ce	Log Qe	Ln Qe	Log Ce	Ln Ce	Ce/Qe
0	0	0	0	0	0	0	0	0	0	0
250	47.79	202.21	0.004	0.0209	0.0049	1.6793	3.8668	2.3058	5.3093	4.2312
500	50.74	449.26	0.002	0.0197	0.0022	1.7053	3.9267	2.6524	6.1076	8.8541
750	55.58	694.42	0.001	0.0179	0.0014	1.7449	4.0178	2.8416	6.5430	12.4940
1000	58.03	941.97	0.001	0.0172	0.0010	1.7636	4.0609	2.9740	6.8479	16.2324

Table 2: Langmuir, Freundlich and Temkin Isotherm Constants for the Adsorption of Cr (VI) ion into *T. indica*

Langmuir		Freundlich		Temkin	
b(L/mg)	0.01286	1/n	0.1279	A_T (L/g)	5.455
q_m (mg/g)	62.118	N	7.8186	b_r	348.994
R_L	0.27 to 0.07	K_f (mg/g)	23.92	B (J/mol)	6.714
R^2	0.99523	R^2	0.92408	R^2	0.9108

3.5 Adsorption Kinetics

The rate of adsorption and the potential rate controlling steps were calculated using an adsorption kinetics experiment. The kinetics were applied for a complete range of contact time studied for different metal ion concentrations. Elovich kinetic models were applied to the experimental data to calculate the Pseudo first and second order kinetics (Chien et al., 1980). Lagergren pseudo-first-order model assumes that the number of unoccupied sites on the surface of the adsorbent at any time is proportional to the rate of occupation of sorption sites i. e., the difference between the saturation concentration of metal ion and solid uptake with time is proportional to the rate of change of solute uptake with time (Cruz et al. 2004; Antunes et al. 2003),. The applicability of Langergren pseudo first order kinetics is shown by a linear plot of log(q_e - q_t) versus t (Lagergren 1898; Ho and McKay 1998). The slope and intercept of the graph gives the rate constant k_t and the equilibrium amount of metal ion q_e.

The first order equation is given by equation 7.

The general form of this model is given by

$$\frac{dq_t}{dt} = k_1(q_e - q_t)$$

where q_e is the mass of metal ions adsorbed at equilibrium (mg/g); q_t is the mass of metal adsorbed at time t (mg/g); k_1 is the first order reaction rate constant (min^{-1}). The integrated equation is written in the form of

$$\frac{q_t}{q_e} = 1 - e^{(-k_1 t)} \quad \text{Or} \quad ln\,(q_e - q_t) = ln\, q_e - k_1 t \qquad (7)$$

From the plot, the value of $k_1$was 0.0019 min^{-1} and the value of q_e, the equilibrium amount of metal ion was 524.468 mg/g. The correlation coefficient for pseudo first order kinetics was 0.9746.

The Ho second order kinetics is based on sorption capacity of solid phase and is calculated from equation 8 (Ho and McKay 1999). Plot of t/q_t vs t gives the kinetic data such as rate constant k_2 and the equilibrium amount of metal ionq_e.

The values k_2 and q_e can be obtained from the slope and the intercept of plot. The general form of pseudo-second-order model is given by

$$\frac{dq_t}{dt} = k_2(q_e - q_t)^2$$

where k_2 is the pseudo-second-order adsorption rate constant ($gmg^{-1}min^{-1}$). The integrated equation is written in the form of

$$\frac{t}{q_t} = \frac{1}{k_2 q_e^2} + \frac{t}{q_e} \quad (8)$$

The value of k_2 and q_e was calculated as 0.1899 g. mg^{-1}. min^{-1} and 20.487 mg. g^{-1} respectively. The correlation coefficient for pseudo second order kinetics was 0.9988. Both pseudo first order and second order curves show linear relation, but the correlation coefficient for pseudo second order kinetics was higher and it can be concluded that the adsorption process follows pseudo second order kinetics.

The elvolich equation has been used in adsorption kinetics for describing the nature of chemical adsorption mechanism (Wu et al. 2009). The general elvolich equation is given by

$$\frac{dq_t}{dt} = \alpha \exp(-\beta q_t)$$

Where α and β are constants. The constant α represents initial adsorption rate (mg. g^{-1}. min^{-1}) because (dq_t/dt) approaches α, when q_t approaches 0, β is desorption constant (g. mg^{-1}) during any experiment. The integrated form of elvolich equation is given in equation 9.

$$q_t = \frac{1}{\beta}\ln(\alpha\beta) + \frac{1}{\beta} \ln t \quad (9)$$

A plot of $q_t$vs ln t should give a linear relationship for the applicability of Elovich kinetics. The correlation coefficient was found as 0.98023. The α and β values were calculated from the slopes and intercepts of the graph as 97.53 mg. g^{-1}. min^{-1} and 0.01752 g. mg^{-1}. The validity of Elvolich model is less compared to Pseudo second order kinetics which can be observed by the low correlation coefficient.

The parameters and constants of Pseudo first-order, second order and Elvolich adsorption kinetics are presented in table 3.

Table 3: Parameters and Constants of Pseudo First-Order, Second Order and Elvolich Adsorption Kinetics

Pseudo First Order		Pseudo Second Order		Elvolich	
q_e(mg. g^{-1})	524.468	q_e(mg. g^{-1})	20.487	α(mg. g^{-1}. min^{-1})	97.53
k_1 (min^{-1})	0.0019	k_2(g. mg^{-1}. min^{-1})	0.1899	β(g. mg^{-1})	0.01752
R^2	0.9746	R^2	0.9988	R^2	0.98023

Figure 4 represents all the adsorption isotherm curves and kinetic curves i. e., adsorption isotherms (a) Langmuir adsorption isotherm, (b) Freundlich adsorption isotherm, (c) Temkin adsorption isotherm and adsorption kinetics (d) Pseudo first order kinetics, (e) Pseudo second order kinetics(f) Elvolich model.

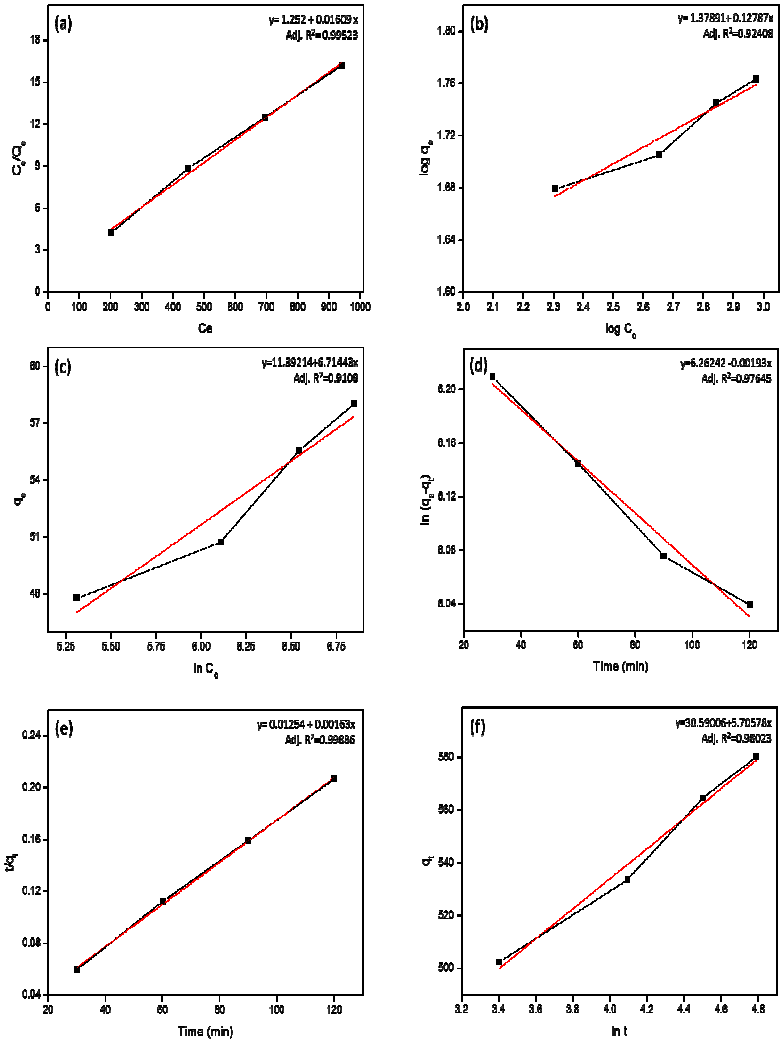

Figure 4: Adsorption Isotherms and Kinetics: (a) Langmuir Adsorption Isotherm Plot between C_e and Ce/q_e; (b) Freundlich Adsorption Isotherm Plot between log $C_e$log q_e; (c) Temkin Adsorption Isotherm Plot between ln C_e and ln q_e;(d) Pseudo First Order Rate Kinetics Plot between Time (min) and log ($q_e - q_t$);(e) Pseudo Second Order Rate Kinetics Plot between Time (min) and t/q_t; (f) Elvolich Plot between ln t and q_t.

On combating the biosorption efficiency of different studies reported previously, it could be observed that *P. emblica* has a considerable potential in the removal of chromium ions. The comparison table is presented in table 3. Since the study deals with real time effluents, the adsorbent can be evaluated for its potential in remediation of industrial effluents on a larger scale. Further the initial ion concentration and amount of adsorbent used are important parameters for calculating q_{max}(maximum biosorption capacity). The value of q_{max} increases with increasing initial ion concentration. In the present study the initial ion concentration was varied from 250 to 1000 mg/L and the adsorbent concentration was high (1g/100mL).

Table 4: Comparison of q_{max} (Biosorption Capacity) value of Different Biosorbents for Chromium Adsorption

Biosorbent	q_{max}(Biosorption Capacity) (mg/g)	Reference
Olive cake	33.44 for Cr (VI)	Dakiky et al. 2002
Terminalia arjuna nuts activated carbon	28.4for Cr (VI)	Mohanty et al. 2005
Neem leaves	62.97for Cr (VI)	Babu and Gupta 2008
Bael fruit shell activated carbon	17.27for Cr (VI)	Anandkumar and Mandal 2009
Orange peel	39.11for Cr (VI)	Bellu et al. 2010
Neem sawdust	58.82for Cr (VI)	Vinodhini and Das2010
Potato peel waste	8.012for Cr (VI)	Abdullah and Prasad 2009
Pine needles	40.0for Cr (VI)	Hadjmohammadi et al. 2011
Osage Orange	93.67for Cr (VI)	Pehlivan et al. 2012
Portulaca Plant biomass	54.95for Cr (VI)	Mishra et al. 2015
Coconut fibre	19.21for Cr (III) &9.54 for Cr (VI)	Henryk et al. 2016
Chitosan microfibers with polyphenols	20.90 for Cr (III)	Zhang et al. 2017
Phyllanthus emblica	62.118	Present study

4. CONCLUSIONS

The present study evaluated the efficiency of *Phyllanthus emblica* leaves in adsorption of Chromium from real time effluents. Various process parameters such as pH, initial adsorbent and adsorbate concentration and contact time were optimized. The adsorption was found to be stable over time. The plant material acted as a sieve for adsorption of chromium ions from real time effluents, which could be observed in SEM images. Further FTIR spectra of the plant material before and after adsorption clearly depicts that chromium ion have been adsorbed by the Cr-O bonds in the spectra. The q_{max} was calculated as 62.118 mg/g for *P. emblica* which was above par compared to previous reports. However, comparing to previous reports, the concentration of chromium ions in the present study is significantly high. Further the adsorption was found to follow Langmuir isotherm and Pseudo second order kinetics. The results indicate that the leaves of *Phyllanthus emblica* are potential adsorbents for chromium ions from real time effluents on a larger scale.

REFERENCES

1. *Balan C, Bilba D, Macoveanu M. Studies on chromium (III) removal from aqueous solutions by sorption on Sphagnum moss peat. J Serb Chem Soc. 2009. 74(8-9):953–964*
2. *Aksu, Z. and D. Akpinar. Competitive biosorption of phenol and chromium (VI) from binary mixtures onto dried anaerobic activated sludge. Biochem. Eng. Jou., 2001.7: 183-193.*
3. *Chwastowski J, Kolozcek H. The kinetic reduction of Cr(VI) by yeast Saccharomyces cerevisiae, Phaffia rhodozyma and their protoplasts. Acta Biochim Pol. 2013. 60(4): 829-824.*
4. *Yuan P, Liu D, Fan M, Yang D, Zhu R, Ge F. Removal of hexavalent chromium [Cr(VI)] from aqueous solutions by the diatomite-supported/unsupported magnetite nanoparticles. J Hazard Mater.2010. 173:614–621.*
5. *Stearns, D. M., & Wetterhahn, K. E. Reaction of chromium(VI) with ascorbate produces chromium(V), chromium (IV), and carbon-based radicals. Chemical Research in Toxicology.1994. 7(2), 219-230.*
6. *Lay, P., Levina, A. Chromium. In A. G. Webb (Eds.), Comprehensive Coordination Chemistry II : From Biology to Nanotechnology [Volume 4: Transition Metal Groups 3-6], (pp. 313-413). 2004*
7. *Hadjmohammadi MR, Salary M, Biparva P. Removal of Cr(VI) from aqueous solution using pine needles powder as a biosorbent. J Appl Sci Environ Sanit. 2011. 6(1):1–13*

8. *Gebrehawaria G, Hussen A, Rao VM, Removal of hexavalent chromium from aqueous solutions using barks of Acacia albida and leaves of Euclea schimperi. Int. J. Environ. Sci. Technol, 2014, 12(5): 1569–1580*
9. *Oboh, I. O., Aluyor, E. O. Luffa cylindrica - an emerging cash crop. African J. Agric. Res.2009. 4 (8): 684-688*
10. *N. Fiol, C. Escudero, I. Villaescusa, Chromium sorption and Cr(VI) reduction to Cr(III) by grape stalks and yohimbe bark, Bioresour. Technol., 2008. 9:5030–5036*
11. *Gupta, S. C., Mishra, M., Sharma, A., Deepak Balaji, T. G., Kumar, R., Mishra, R. K., Chowdhuri, D. K. Chlorpyrifos induces apoptosis and DNA damage in Drosophila through generation of reactive oxygen species. Ecotoxicol. Environ. Saf. 2010. 73(6): 1415--1423*
12. *S. Pehlivan, O. Ovayolu, N. Ovayolu, A. Sevinc, C. Camci. Relationship between hopelessness, loneliness, and perceived social support from family in Turkish patients with cancer. Supportive Care in Cancer.2012. 20(4):733-739*
13. *Farooq M, Wahid A, Lee DJ, Cheema SA, Aziz T. Comparative time course action of the foliar applied glycinebetaine, salicylic acid, nitrous oxide, brassinosteroids and spermine in improving drought resistance of rice. J. Agron. Crop Sci. 2010. 196: 336-345.*
14. *Garima Mahajan and Dhiraj sud. Kinetics and equilibrium studies of Chromium (VI) metal ion remediation by on Archias hypogeal shells: A green approach. Bioresources. 2011. 6(3):3324-3338.*
15. *Azouaoua N, Sadaouia Z, Djaafri A, Mokaddema H. Adsorption of cadmium from aqueous solution onto untreated coffee grounds: equilibrium, kinetics and thermodynamics. J Hazard Mater.2010. 184(1–3):126–134.*
16. *Misra S, Mandal N and Dasgupta S. Role of pressure and temperature in inclusion-induced shear localization: An analogue experimental approach. Jour of Structural Geology. 2015. 81 78-88*
17. *E. Malkoc, Y. Nuhoglu, Y. Abali. Cr(VI) adsorption by waste acorn of Quercus ithaburensis in fixed beds: Prediction of breakthrough curves. Chem. Eng. J, 2006. 119: 61–68*
18. *Reddy, A. C. Low and High Temperature Micromechanical Behavior of BN/3003 Aluminum Alloy Nanocomposites.*
19. *Ucun, H., Bayhan, Y. K., Kaya, Y., Cakici, A. and Algur, O. F. Biosorption of chromium (VI) from aqueous solution by cone biomass of Pinus sylvestris', Bioresource Technology. 2002. 85(2):155–158.*
20. *Dakiky, M., Khami, A., Manassra, A. and Mer'eb, M. Selective adsorption of chromium (VI) in industrial wastewater using low cost abundantly available adsorbents. Advances in Environmental Research. 2002. 6(4): 533–540.*
21. *V. K. Garg, R. Kumar, R. Gupta. Removal of malachite green dye from aqueous solution by adsorption using agro-industry waste: a case study of Prosopis cineraria. Dyes Pigm., 2004. 62:1-5*
22. *S. Babel and E. M. Opiso. Removal of Cr from synthetic wastewater by sorption into volcanic ash soil. Int. J. Environ. Sci. Tech. 2007. 4(1):99-107.*
23. *Mezenner YN, Bensmaili A. Kinetics and thermodynamic study of phosphate adsorption on iron hydroxide-eggshell waste. Chem. Eng. J. 2009. 147:87–96.*
24. *Kaouah, F., Boumaza, S., Berrama, T., Trari, M., Bendjama, Z., 2013. Preparation and characterization of activated carbon from wild olive cores (oleaster) by H3PO4 for the removal of basic red 46. J. Clean. Prod. 2013. 54:296-306.*
25. *Abdullah, M. A. and A. G. D. Prasad: Kinetic and equilibrium studies for the biosorption of Cr(VI) from aqueous solutions by potato peel waste. Int. J. Chem. Eng. Res., 2009. 1(2), 51–62.*

26. *Chien, S. H. and W. R. Clayton: Application of Elovich equation to the kinetics of phosphate release and sorption on soils. Soil Sci. Soc. Am. 1980. 44: 265-268*
27. *Ho, Y. S. and G. Mckay: Kinetic model for lead (II) sorption on to peat. Adsorption. Science and Technology. 1998. 16 (4): 243-255.*
28. *Nagaral, M., Auradi, V., & Ravishankar, M. K. (2013). mechanical behaviour of aluminium 6061 alloy reinforced with al2o3 & graphite particulate hybrid metal matrix composites. International Journal of Research in Engineering & Technology (IJRET) Vol, 1, 193-198.*
29. *Ho, Y. S. and G. Mckay: A kinetic study of dye sorption by Biosorbent waste product pith. Resources Conservation and Recycling. 25 (3-4): 171-193.*
30. *Temkin, M. I. and V. Pyzhev: Kinetics of ammonia synthesis on promoted iron catalyst. Acta Phys. Chim.1940. 12: 327–356*
31. *Voudrias, E., F. Fytianos and E. Bozani: Sorption description isotherms of dyes from aqueous solutions and waste waters with different sorbent materials. Global Nest, The Int. J. 2002. 4(1):75-83*
32. *Gebrehawaria, G., Hussen, A. and Rao, V. M. Removal of hexavalent chromium from aqueous solutions using barks of Acacia albida and leaves of Euclea schimperi. Int. J. Environ. Sci. Technol. 2015. 12 (5), 1569–1580*
33. *Muthulakshmi A., Baskaran R. and Ashwin karthick N. Removal of Chromium from Aqueous Solution Using Tamarindus indica Leaves as Adsorbent. Journal of Environmental Biology. 2016. 37 (6):1443-1450*
34. *Muthulakshmi A., Baskaran R. and Ashwin Karthick N. Adsorption studies of Hexavalent Chromium using Syzygium cumini bark, Journal of Chemical and Pharmaceutical Sciences. 2016. 9 (3): 1442-1445.*
35. *Muthulakshmi A., and Baskaran R. Adsorption of Hexavalent Chromium in Industrial Water Using Pithecellobium Dulce Bark, Research Journal of Pharmaceutical, Biological and Chemical Sciences. 2017. 8 (1): 1450-1456*
36. *Cruz, N., Figueiredo, S., Viana da Fonseca, A. Deriving relic structure parametrical evidences by interpreting DMT+CPT(U)+lab tests. Geotechnical & Geophysical Site Characterization. Proc. 2nd Int. Site Characterization - ISC'2, Porto, Portugal, Sept. 2004.*
37. *Reddy, A. C. (2015). Studies on loading, cracking and clustering of particulates on the strength and stiffness of 7020/SiCp metal matrix composites. International Journal of Metallurgical & Materials Science and Engineering, 5(1), 53-66.*
38. *Antunes DF, et al. Motifs in Schizosaccharomyces pombe ars3002 important for replication origin activity in Saccharomyces cerevisiae. Plasmid. 2013. 50(2):113-119*
39. *Lagergren, S. Zur theorie der sogenannten adsorption gelöster stoffe, Kungliga Svenska Vetenskapsakademiens. Handlingar. 1898. 24 (4) : 1.39.*
40. *Wu Y, et al. Welcome the family of FANCJ-like helicases to the block of genome stability maintenance proteins. Cell Mol Life Sci. 2009. 66(7):1209-22*